Anisotropic thermal expansion in rare earth intermetallic compounds RZn_2 with R=Gd, Tb and Dy

1995 J. Phys.: Condens. Matter 7 6809

(http://iopscience.iop.org/0953-8984/7/34/006)

J. Phys.: Condens. Matter 7 (1995) 6809–6821. Printed in the UK

Anisotropic thermal expansion in rare earth intermetallic compounds RZn_2 with R = Gd, Tb and Dy

S Ohta†, T Kitai‡ and T Kaneko§

† Hachinohe Institute of Technology, Hachinohe-shi, Aomori 031, Japan

‡ Department of Applied Physics, Kyushu Institute of Technology, Tobata-ku, Kitakyushu-shi 804, Japan

§ Institute for Materials Research, Tohoku University, Sendai-shi, Miyagi 980, Japan

Received 13 February 1995, in final form 12 May 1995

Abstract. We have measured the lattice parameters $a(T)$, $b(T)$ and $c(T)$ as a function of temperature T in the range 15 K < T < 300 K for RZn_2 (R = Gd, Tb or Dy) with the $CeCu_2$-type crystal structure. Anisotropic thermal expansion is observed in the $a(T)$, $b(T)$ and $c(T)$ against T plots for all materials investigated below the magnetic transition temperatures T_{tr}. The linear expansivity above T_{tr} along the b direction becomes small on varying the rare earth atom R in RZn_2 from R = Gd to Dy to Tb. The sign of the change in c, $\Delta c/c$, for $GdZn_2$ below T_{tr} is positive while those for $TbZn_2$ and $DyZn_2$ are negative. The cell volume in all materials expands when magnetic orderings appear. The obtained results are qualitatively understood in terms of the phenomenological model in which the crystal field and magnetic exchange contributions to the thermal expansion are taken into account.

1. Introduction

Rare earth (R) intermetallic compounds RZn_2 (R = Gd, Tb and Dy) crystallize in the orthorhombic $CeCu_2$-type structure [1] in which the R atoms occupy the 4e sites and the Zn atoms the 8h ones, as shown in figure 1(a). As one of the features in this structure, R atoms form a zig-zag chain along the b axis which is doubly separated by Zn layers (figure 1(b)). Since the atomic arrangement of R atoms in the $CeCu_2$-type structure has a low-dimensional character, it appears that the crystal field around R atoms for the orthorhombic symmetry is different from that for the cubic one.

For the measurements of magnetization and magnetic susceptibility against temperature (T), $GdZn_2$ is ferromagnetic with the Curie temperature T_C = 68 K [2] while $TbZn_2$ and $DyZn_2$ are antiferromagnetic with the Néel temperatures T_N = 75 K [3] and 35 K [4], respectively. The paramagnetic Curie temperatures θ_p for polycrystalline samples of RZn_2 with R = Ce–Tm are positive even though the materials are antiferromagnetic [4]. Such a magnetic behaviour has been understood on the basis of the Rudermann–Kittel–Kasuya–Yosida (RKKY) theory [4]. Neutron diffraction study [5] for single-crystal $DyZn_2$ has revealed that the magnetic moments for Dy at 4.2 K are ferromagnetically aligned within the basal plane and antiferromagnetically stacked along the c direction. In $DyZn_2$, the magnetic moment of Dy at 4.2 K is 9.7 μ_B [5] which is close to that expected for a tripositive free ion Dy^{3+}. The values of θ_p for the a and b axes in a single crystal of $DyZn_2$ are positive while that for the c axis is negative [6]. This implies that the crystal field effect plays an important role in anisotropic magnetic properties of RZn_2, which is similar to that in the case [7, 8] of RCu_2.

0953-8984/95/346809+13$19.50

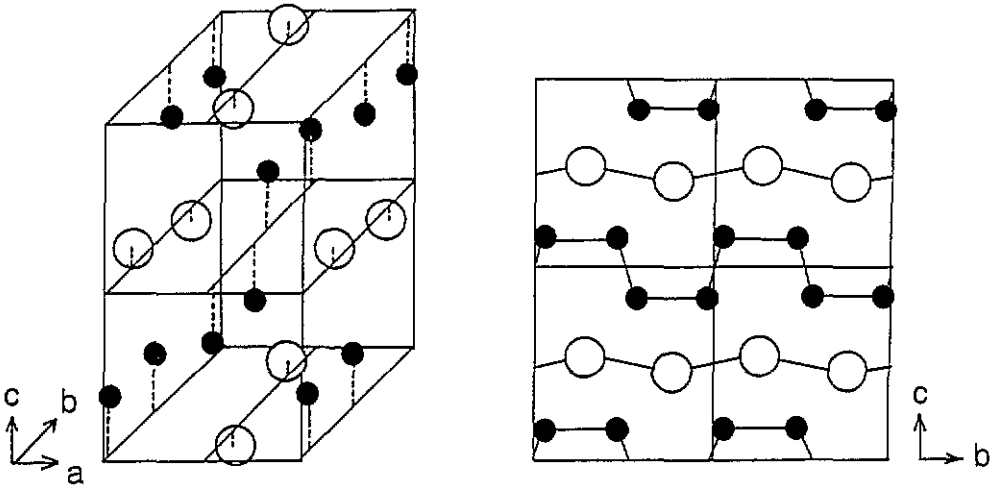

Figure 1. (a) The unit cell of the orthorhombic $CeCu_2$-type crystal structure and (b) the atomic arrangement of the rare earth and zinc atoms in the b–c plane, in which four unit cells are depicted. Here, open and closed circles indicate the rare earth and zinc atoms, respectively.

Recently, the influence of the crystal field on the anisotropic thermal expansion in RCu_2 (R = Nd [9, 10], Sm [11], Er [10, 12] and Tm [12, 13]) with the $CeCu_2$-type structure has been intensively investigated from the viewpoint of the relation between magnetic properties and the crystal field effect. The anisotropic thermal expansion behaviour above the magnetic transition temperature was well explained in terms of the temperature behaviour of the thermal average of the second-order crystal field parameters. In RZn_2 (R = Gd, Tb or Dy), the values of a and b among the lattice parameters a, b and c at room temperature decrease with varying R from R = Gd to Tb to Dy while that of c hardly depends on R [14]. On the other hand, all values of a, b and c in RCu_2 with R = Gd, Tb or Dy decrease with varying R [15]. The variation of c with R in RZn_2 is strikingly different from that in the case of RCu_2. This suggests that the crystal field effect on magnetic properties in RZn_2 with Tb and Dy is strongly correlated to the crystallographic character along the a, b or c direction. It is of interest to investigate the origin of the appearance of various magnetic ordering in RZn_2 from the viewpoint of the crystal field effect on the thermal expansion. So far, magnetic properties of RZn_2 have been extensively investigated. However, little is known of the thermal expansion behaviour for RZn_2 from the above point of view, in comparison with the case of RCu_2. The purpose of the present paper is to present the preliminary measurement on the thermal expansion for RZn_2 (R = Gd, Tb or Dy) and to present a simple expression on the basis of the phenomenological model in order to explain the obtained results.

2. Experimental procedures

Polycrystalline samples were prepared in the same way as reported previously [5]. The values of a, b and c and cell volume V at room temperature are summarized in table 1. These values are consistent with the reported ones [14]. The measurement of $a(T)$, $b(T)$

and $c(T)$ at various temperatures was carried out in the temperature range between 18 K and about 300 K using a powder x-ray diffraction method with graphite-monochromatized Cu Kα radiation. The temperature was controlled to within ± 0.2 K using a silicon diode thermometer attached close to the sample and using a helium gas closed cycle refrigerator. In order to calibrate the scattering angle in the present experiment, the sample was well mixed with Si powder (99.99% pure) as an internal standard whose thermal expansion was taken from [16].

Table 1. Values of lattice parameters a, b, and c and cell volume V for RZn_2 (R = Gd, Tb and Dy).

RZn_2	a (Å)	b (Å)	c (Å)	V (Å^3)
$GdZn_2$	4.5094	7.2280	7.5907	247.41
$TbZn_2$	4.4897	7.1468	7.5927	243.62
$DyZn_2$	4.4720	7.0880	7.5951	240.75

The coefficient of the linear thermal expansion α_L ($L = a$, b or c) is estimated by the least-squares fitting for a linear equation $L(T) = f + gT$ in the temperature interval about 30 K and by differentiating $L(T)$ with respect to T. Here f and g are the fitting parameters. The value of the volumetric expansivity β is similarly estimated in the same way as that of α_L.

3. Results

The temperature dependences of $a(T)$, $b(T)$ and $c(T)$ for $GdZn_2$ are shown in figure 2. As T increases, $a(T)$ increases up to about 60 K and then more gradually increases up to about 300 K. A feeble kink around 60 K is observed on the temperature derivative of c, dc/dT, against T plots within the experimental accuracy. On the other hand, $b(T)$ and $c(T)$ decrease up to about 60 K above which both increase smoothly up to about 300 K. The temperature where the $b(T)$ and $c(T)$ against T plots exhibit a minimum around about 60 K corresponds well to the reported value [2] of T_C (= 68 K). Hence, it is considered that the anomalous thermal expansion below about 60 K is due to the appearance of ferromagnetic ordering. From this, the value of T_C is determined to be (60 ± 2) K. Below T_C, the relative change in a below and above T_C, $\Delta a/a$, is small and negative while those in b and c are both large and positive. Here, $\Delta L/L$ ($L = a$, b and c) represents the change in lattice parameter at 0 K and is defined by the following expression:

$$\Delta L/L = [L_0(T < T_C) - L_0(T > T_C)]/L_0(T > T_C)$$

where $L_0(T < T_C)$ and $L_0(T > T_C)$ are estimated from the straight extrapolation line from the ferromagnetic state ($T < T_C$) and the paramagnetic one ($T > T_C$) to 0 K, respectively. From the results of $L(T)$ ($L = a$, b or c) in the temperature range above T_C, the values of α_a, α_b and α_c above T_C are summarized in table 2. As seen in figure 3, $V(T)$ decreases with increasing T up to about 60 K and then increases linearly. The value of β above T_C is also given in table 2.

Figure 4 shows the temperature dependences of $a(T)$, $b(T)$ and $c(T)$ for $TbZn_2$. As seen in the figure, $a(T)$ for $TbZn_2$ decreases up to about 55 K and then increases up to about 85 K with increasing T. Above about 85 K, $a(T)$ increases more slowly with increasing T. The temperature where the $a(T)$ against T plots exhibit a minimum around about

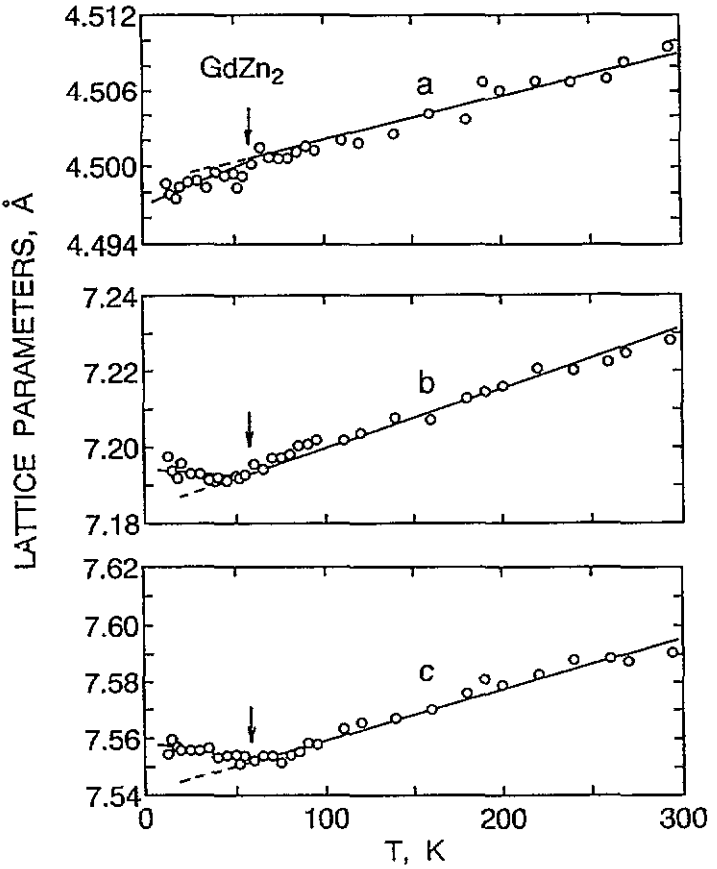

Figure 2. The temperature dependences of lattice parameters a, b and c for $GdZn_2$. The downward arrows indicate T_C. The solid lines are guides for the eye.

Table 2. Values of linear thermal expansivity for the principal axes, α_a, α_b and α_c, and volumetric expansivity β for RZn_2 (R = Gd, Tb and Dy). Units are 10^{-5} K^{-1}.

RZn_2	α_a	α_b	α_c	β
$GdZn_2$	0.85 ± 0.03	1.94 ± 0.03	2.39 ± 0.01	5.18 ± 0.08
$TbZn_2$	0.64 ± 0.04	0.53 ± 0.02	2.03 ± 0.04	3.20 ± 0.05
$DyZn_2$	0.90 ± 0.03	0.98 ± 0.04	2.24 ± 0.04	4.12 ± 0.08

55 K corresponds well to the value of T_t (= 60 K) where the magnetic structure changes from a linear transverse sinusoidal spin structure to an antiferromagnetic one in a neutron diffraction study [3]. Furthermore, one can see a kink around about 85 K on the $a(T)$ against T plots. According to the preliminary measurement of magnetic properties [17] for single-crystal $TbZn_2$, a sharp peak around 85 K was observed on the magnetic susceptibility against T plots. This peak was assigned to the Néel temperature. Therefore, it is considered that the temperature where $da(T)/dT$ changes around about 85 K corresponds to the value of T_N. As T increases, $b(T)$ decreases up to about 85 K and then increases up to about 300 K. However, a feeble kink around about 55 K and 85 K is observed on the $dc(T)/dT$ against T plots. Above about 90 K, $c(T)$ increases monotonically up to about 300 K. Then,

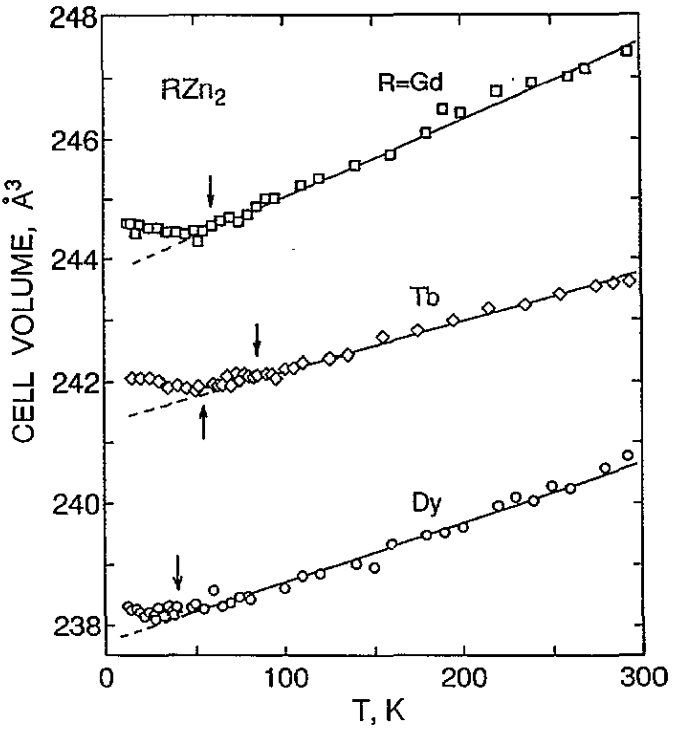

Figure 3. The temperature dependence of cell volume for RZn_2 with R = Gd, Tb and Dy. The downward and upward arrows indicate T_C or T_N and T_t, respectively. The solid lines are guides for the eye.

the values of T_t and T_N are determined to be (55 ± 2) K and (85 ± 2) K, respectively, in the present study. In the range $T < T_t$, the signs of $\Delta a/a$ and $\Delta c/c$ are negative while that of $\Delta b/b$ is positive. The values of α_a, α_b and α_c above T_N for $TbZn_2$ are summarized in table 2. As T increases, $V(T)$ for $TbZn_2$ decreases up to about 55 K and then increases up to about 85 K (figure 3). Around 85 K, a feeble kink is observed on the $V(T)$ against T plots. As T further increases, $V(T)$ increases up to about 300 K. The value of β above T_N for $TbZn_2$ is also given in table 2.

Figure 5 shows the temperature dependences of $a(T)$, $b(T)$ and $c(T)$ for $DyZn_2$. As T increases, $a(T)$ and $b(T)$ both decrease up to about 40 K and then increase linearly up to about 300 K. On the other hand, $c(T)$ increases steeply with increasing T up to about 40 K and then increases more slowly up to about 300 K. The temperature where the $a(T)$, $b(T)$ and $c(T)$ against T plots exhibit a kink around about 40 K corresponds well to the value of T_N (= 38 K [3]). Then, it is considered that the anomalous thermal expansion is due to the appearance of antiferromagnetic ordering. In the present study, the value of T_N is determined to be (40 ± 2) K. For $T < T_N$, the signs of $\Delta a/a$ and $\Delta b/b$ are positive while that of $\Delta c/c$ is negative. As seen in figure 3, $V(T)$ for $DyZn_2$ decreases with increasing T up to about 40 K and then it increases with increasing T. The values of α_a, α_b and α_c and β above T_N are summarized in table 2.

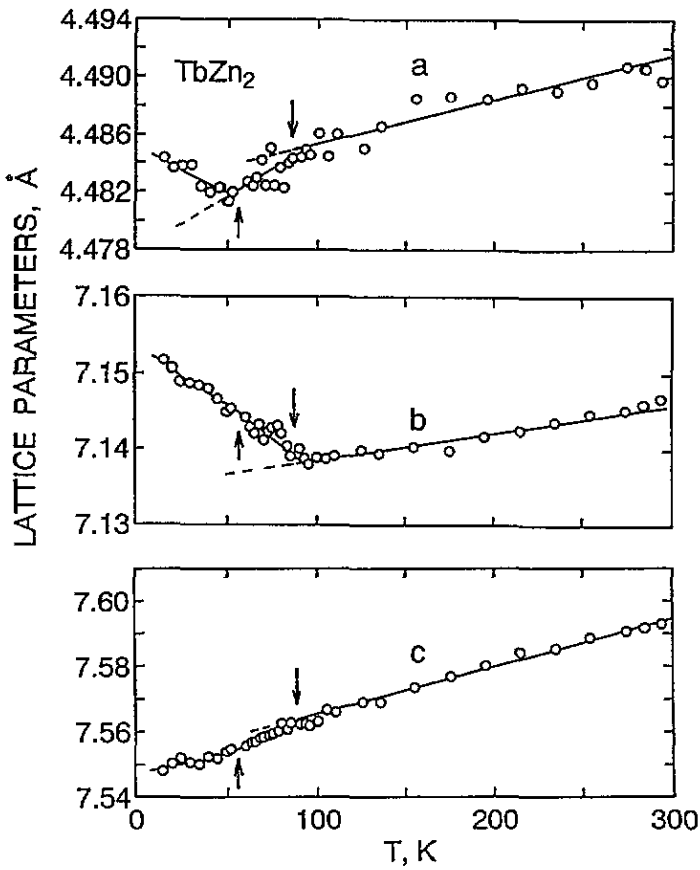

Figure 4. The temperature dependences of lattice parameters a, b and c for $TbZn_2$. The downward and upward arrows indicate T_N and T_t, respectively. The solid lines are guides for the eye.

4. Discussion

4.1. The spatial dependence of exchange interactions

Thermal expansion studies for RCu_2 (R = Nd [9, 10], Sm [11], Er [10, 12], Tm [12, 13]) have demonstrated that the temperature dependence of the b axis is closely connected with the atomic arrangement of the R atoms in this direction, as seen in figure 1(b). In the $CeCu_2$-type structure, the nearest-neighbour distance between R atoms along the b direction, r^b, is shorter than the next-nearest-neighbour ones between R atoms along the a and c directions, r^a and r^c, respectively. Here, r^L ($L = a$, c) and r^b are given by $r^L = [(a/2)^2 + (0.5 - 2\delta)^2 c^2]^{1/2}$ ($L = a$ or c) and $r^b = [(b/2)^2 + (2\delta c)^2]^{1/2}$, respectively, where a, b and c are the values at room temperature and δ represents the difference between a positional parameter z(R) and an ideal position for an R atom and is given by $\delta = z(R) - 0.5$. The evaluated values of r^L ($L = a$, b and c) for RZn_2 (R = Gd, Tb and Dy) are summarized in table 3. Here, the value of z(Dy) (= 0.537) [5] for a Dy atom is used in calculating r^L. As seen in table 3, the value of r^b decreases with varying R in RZn_2 from R = Gd to Tb to Dy while those of r^a and r^c remain nearly constant.

The values of θ_p, as a measure of exchange integral, for polycrystalline samples of RZn_2

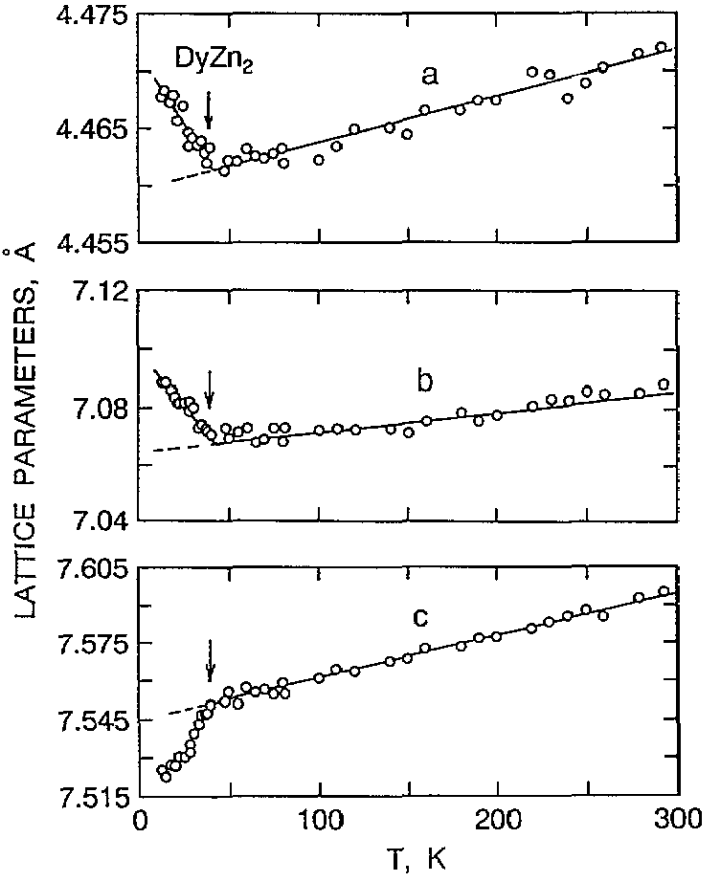

Figure 5. The temperature dependences of lattice parameters a, b and c for $DyZn_2$. The downward arrows indicate T_N. The solid lines are guides for the eye.

Table 3. Values of the nearest-neighbour distance between R atoms along the b direction, r^b, and the next-nearest-neighbour distance between R atoms along the a and c directions, r^a and r^c, respectively, for RZn_2 (R = Gd, Tb and Dy).

RZn_2	r^a or r^c (Å)	r^b (Å)
$GdZn_2$	3.96	3.65
$TbZn_2$	3.95	3.61
$DyZn_2$	3.95	3.59

and RCu_2 are tentatively plotted as a function of r^b, from which we can estimate the spin polarization between R atoms against r. Here, $\theta_p = (\theta_p^a + \theta_p^b + \theta_p^c)/3$ where θ_p^L ($L = a$, b or c) refers to the paramagnetic Curie temperatures along each principal axis. The inset of figure 6 shows the values of θ_p for RCu_2 as a function of r^b, where $z(\mathrm{Ce}) = 0.5377$ [1] in $CeCu_2$ is used in calculating r^b. The data for θ_p and the lattice parameters at room temperature are mainly taken from [7], [8] and [15] except those for $TmCu_2$ [13]. As seen from the θ_p against r plots for RCu_2, the sign of θ_p varies from positive to negative as

r increases. Similarly, the values [2,3] of θ_p against r^b for RZn_2 are plotted in the same figure (see the inset of figure 6). The value of θ_p for RZn_2 increases up to that for $GdZn_2$ (θ_p = 70 K; r^b = 3.65 Å) and then decreases with increasing r^b. It is noted that the up–down behaviour of θ_p for RZn_2 against r is remarkably different from that for RCu_2. From the θ_p–r plots for RZn_2, the ferromagnetic exchange interaction couples with R atoms in the same distance range 3.5 Å < r < 3.9 Å and its magnitude is strongly spatially dependent on the distance between R atoms along the b direction. In comparison with the θ_p–r plots for RCu_2, the up–down behaviour in RZn_2 implies that the RKKY interaction has a predominant role in the magnetic properties of RZn_2. Under these situations, the positive thermal expansion along the b direction in all cases of RZn_2 investigated is expected in the temperature range below T_{tr}.

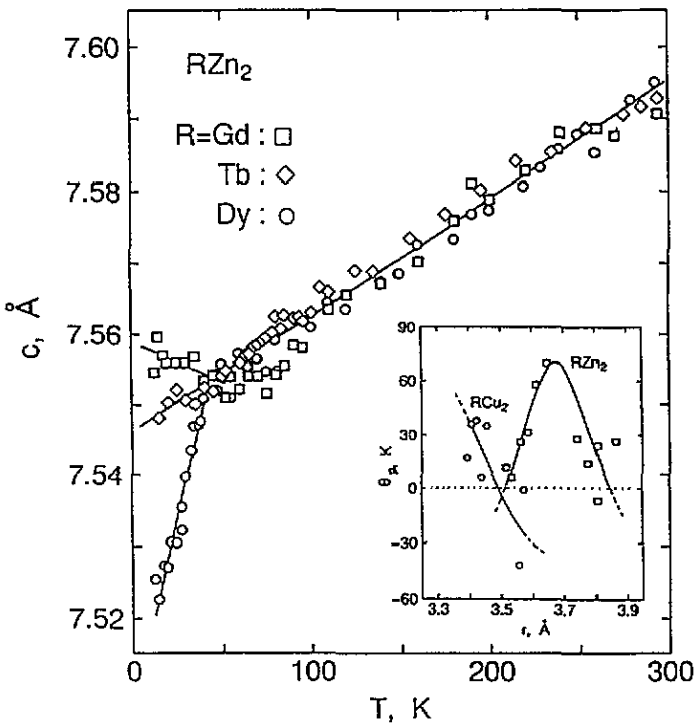

Figure 6. The temperature dependence of lattice parameters c for RZn_2 with R = Gd, Tb and Dy. The inset shows the paramagnetic Curie temperature θ_p for polycrystalline samples of RCu_2 (open circles) and RZn_2 (open squares) as a function of distance r. Data for RCu_2 and RZn_2 are mainly taken from [7] and [8], and [4], respectively. The solid lines are guides for the eye.

4.2. The phenomenological model

In the previous studies [9–13] of the thermal expansion in RCu_2, it has been shown that the thermal expansion in the paramagnetic temperature range is well explained in terms of the contributions originating form the crystal field and magnetoelastic interactions. First, we describe the crystal field and magnetoelastic Hamiltonians and elastic energy which are similar expressions to those proposed in the previous studies [9–13] of thermal expansion for RCu_2. In the unstrained lattice, the crystal field (CF) Hamiltonian H_{CF} is [18]

$$H_{CF}(\varepsilon = 0) = V_2^0 O_2^0(J) + V_2^2 O_2^2(J) + V_4^0 O_4^0(J) + V_4^2 O_4^2(J) + V_4^4 O_4^4(J) + V_6^0 O_6^0(J)$$

$$+V_6^2 O_6^2(J) + V_6^4 O_6^4(J) + V_6^6 O_6^6(J) \tag{1}$$

where V_i^J and O_i^m are the crystal field parameters and the Steven's operator equivalents with the total angular momentum quantum number J, respectively. In the strained lattice, the one-ion magnetoelastic (me) Hamiltonian H_{me} [19] for orthorhombic symmetry is

$$H_{me}(\varepsilon) = \varepsilon_1(B_{10}^1 O_2^0 + B_{11}^1 O_2^2) + \varepsilon_2(B_{20}^1 O_2^0 + B_{21}^1 O_2^2) + \varepsilon_3(B_{30}^1 O_2^0 + B_{31}^1 O_2^2) + B^2\varepsilon_4(J_1 J_2 + J_2 J_1) + B^3\varepsilon_5(J_1 J_3 + J_3 J_1) + B^4\varepsilon_6(J_2 J_3 + J_3 J_2) \tag{2}$$

where B_{i0}^1, B_{i1}^1, B^2, B^3, B^4 are the magnetoelastic coupling parameters, ε_i (i = 1–6) the component of the strain tensor and J_i the components of the total angular momentum operator. Within the harmonic hypothesis, the elastic (el) energy F_{el} is written [20] as

$$F_{el}(\varepsilon) = \tfrac{1}{2}(c_{11}\varepsilon_1^2 + c_{22}\varepsilon_2^2 + c_{33}\varepsilon_3^2) + c_{12}\varepsilon_1\varepsilon_2 + c_{13}\varepsilon_1\varepsilon_3 + c_{23}\varepsilon_2\varepsilon_3 + c_{44}\varepsilon_4^2 + c_{55}\varepsilon_5^2 + c_{66}\varepsilon_6^2 \tag{3}$$

where c_{ij} are nine independent elastic constants for the orthorhombic symmetry.

The characteristic minimum as the influence of the crystal field in the paramagnetic temperature range has been observed in the thermal expansion of RCu_2 [9–13]. Such a thermal expansion behaviour was well explained in terms of $H_{CF}(\varepsilon)$, $H_{me}(\varepsilon)$ and $F_{el}(\varepsilon)$. However, a minimum behaviour in $a(T)$, $b(T)$ and $c(T)$ for the present compounds has not been observed in the paramagnetic temperature range. This is the striking difference between the thermal expansion behaviour of RZn_2 investigated presently and that of RCu_2. Although we have not considered the contribution from quadrupole pair interactions to thermal expansion, it has been pointed out that these interactions play an important role in the magnetically ordered state in rare earth equiatomic intermetallic compounds [21]. The crystal symmetry below and above T_{tr} in all RZn_2 investigated is the same as the orthorhombic one. Then, it is considered that the quadrupole pair interactions have a small contribution to the thermal expansion anomaly in the present system. Together with the considerations described in 4.1, the magnetic exchange contribution to the thermal expansion besides the CF and magnetoelastic ones may be important in anisotropic thermal expansion behaviour in RZn_2 (R = Gd, Tb, Dy) below T_{tr}. The magnetic measurements [6, 17] for RZn_2 (R = Tb, Dy, Ho and Er) have revealed that the effective Bohr magneton per R ion is in good agreement with that expected in a respective free-ion value. These situations remind us of the exchangestriction in the localized system. In the present paper, we will propose the most simple expression in order to explain qualitatively the obtained results.

We assume that the anisotropic Heisenberg-type exchange (ex) Hamiltonian H_{ex} may be written as follows:

$$H_{ex}(\varepsilon) = \sum_{nn,1} I_1(\varepsilon_1) S_k \cdot S_l + \sum_{nn,2} I_2(\varepsilon_2) S_k \cdot S_l + \sum_{nn,3} I_3(\varepsilon_3) S_k \cdot S_l \tag{4}$$

where $I_i(\varepsilon_i)$ is the directional- and the strain-dependent exchange integral between R atoms at sites k and l, S_k represents the spin of R at a site k and $\sum_{nn,i}$ refers to summation over all pairs of nearest neighbours (nn) along the i (= 1, 2 and 3) direction. Here, we confine ourselves to consider only the strain along the principal axes. In the small-strain limit, we assume that $I_i(\varepsilon_i)$ (i = 1, 2, 3) may be written, in a similar way to the study [22] of lattice deformation in MnO, as follows:

$$I_1(\varepsilon_1) = I_1(1 - \eta_1\varepsilon_1) \tag{5a}$$

$$I_2(\varepsilon_2) = I_2(1 - \eta_2\varepsilon_2) \tag{5b}$$

$$I_3(\varepsilon_3) = I_3(1 - \eta_3\varepsilon_3) \tag{5c}$$

where I_i represents the exchange integral in the unstrained state and η_i is the dimensionless parameter $\eta_i = -\partial \ln I_i / \partial \ln \varepsilon_i$.

Hence, the total free energy $F_{tot}(\varepsilon)$ as a function of a strain ε below T_{tr} is written as

$$F_{tot}(T, \varepsilon) = F_{me}(T, \varepsilon) + F_{ex}(T, \varepsilon) + F_{el}(\varepsilon) \tag{6}$$

where the first, second and third terms on the right-hand side are the magnetoelastic, exchange and elastic parts of the free energy, respectively. In (6), the magnetoelastic part $F_{me}(T, \varepsilon)$ and the exchange one $F_{ex}(T, \varepsilon)$ may be written in terms of $H_{me}(\varepsilon)$ (2) and $H_{ex}(\varepsilon)$ (4) as

$$\begin{aligned} F_{me}(T, \varepsilon) &= -k_B T \ln[\mathrm{Tr} \exp(-H_{me}(\varepsilon)/k_B T)] \\ F_{ex}(T, \varepsilon) &= -k_B T \ln[\mathrm{Tr} \exp(-H_{ex}(\varepsilon)/k_B T)] \end{aligned} \tag{7}$$

where k_B is the Boltzmann constant. The equilibrium situation can be found by minimizing the total free energy (6) with respect to ε_i. In that case, it is noted that $\partial F_{tot}(\varepsilon)/\partial \varepsilon_i = \langle \partial H_{tot}(\varepsilon)/\partial \varepsilon_i \rangle$, where the angular brackets denote a thermal average over the ensemble. The equilibrium conditions for ε_1, ε_2 and ε_3 are

$$\begin{aligned} &\langle \partial H_{tot}(\varepsilon)/\varepsilon_1 \rangle + \partial F_{el}(\varepsilon)/\partial \varepsilon_1 = 0 \\ &\langle \partial H_{tot}(\varepsilon)/\varepsilon_2 \rangle + \partial F_{el}(\varepsilon)/\partial \varepsilon_2 = 0 \\ &\langle \partial H_{tot}(\varepsilon)/\varepsilon_3 \rangle + \partial F_{el}(\varepsilon)/\partial \varepsilon_3 = 0. \end{aligned}$$

Substituting (1)–(4) yields three simultaneous linear equations in ε_1, ε_2 and ε_3:

$$c_{11}\varepsilon_1 + c_{12}\varepsilon_2 + c_{13}\varepsilon_3 + B^1_{10}\langle O^0_2 \rangle + B^1_{11}\langle O^2_2 \rangle - I_1\eta_1 \left\langle \sum_{nn,1} S_k \cdot S_l \right\rangle = 0 \tag{8a}$$

$$c_{12}\varepsilon_1 + c_{22}\varepsilon_2 + c_{23}\varepsilon_3 + B^1_{20}\langle O^0_2 \rangle + B^1_{21}\langle O^2_2 \rangle - I_2\eta_2 \left\langle \sum_{nn,2} S_k \cdot S_l \right\rangle = 0 \tag{8b}$$

$$c_{13}\varepsilon_1 + c_{23}\varepsilon_2 + c_{33}\varepsilon_3 + B^1_{30}\langle O^0_2 \rangle + B^1_{31}\langle O^2_2 \rangle - I_3\eta_3 \left\langle \sum_{nn,3} S_k \cdot S_l \right\rangle = 0. \tag{8c}$$

These equations may be written in the matrix form:

$$\begin{pmatrix} c_{11} & c_{12} & c_{13} \\ c_{12} & c_{22} & c_{23} \\ c_{13} & c_{23} & c_{33} \end{pmatrix} \begin{pmatrix} \varepsilon_1 \\ \varepsilon_2 \\ \varepsilon_3 \end{pmatrix} = - \begin{pmatrix} B^1_{10}\langle O^0_2 \rangle + B^1_{11}\langle O^2_2 \rangle - I_1\eta_1 \left\langle \sum_{nn,i} S_k \cdot S_l \right\rangle \\ B^1_{20}\langle O^0_2 \rangle + B^1_{21}\langle O^2_2 \rangle - I_2\eta_2 \left\langle \sum_{nn,2} S_k \cdot S_l \right\rangle \\ B^1_{30}\langle O^0_2 \rangle + B^1_{31}\langle O^2_2 \rangle - I_3\eta_3 \left\langle \sum_{nn,3} S_k \cdot S_l \right\rangle \end{pmatrix}. \tag{9}$$

Note that the elastic compliance coefficient κ_{ji} is given [23] as a cofactor of c_{ij}/(determinant of the c); the equilibrium strain for ε_i^{eq} ($i = 1$, 2 and 3) is found to be

$$\begin{aligned} \varepsilon_i^{eq} = &-(\kappa_{i1}B^1_{10} + \kappa_{i2}B^1_{20} + \kappa_{i3}B^1_{30})\langle O^0_2 \rangle - (\kappa_{i1}B^1_{11} + \kappa_{i2}B^1_{21} + \kappa_{i3}B^1_{31})\langle O^2_2 \rangle \\ &+\kappa_{i1}I_1\eta_1 \left\langle \sum_{nn,1} S_k \cdot S_l \right\rangle + \kappa_{i2}I_2\eta_2 \left\langle \sum_{nn,2} S_k \cdot S_l \right\rangle + \kappa_{i3}I_3\eta_3 \left\langle \sum_{nn,3} S_k \cdot S_l \right\rangle \end{aligned} \tag{10}$$

where $\langle O^0_2 \rangle$ and $\langle O^2_2 \rangle$ are the thermal average of O^m_n ($m = 0, 2$; $n = 2$) which has been given in [12]. If ξ_i is the number of nearest neighbours of any particular spin along the

i direction, then we could write $(\sum_{nn,i} S_k \cdot S_l) = \xi_i \langle S_k \cdot S_l \rangle$ $(i = 1, 2, 3)$. Then (10) may be rewritten as

$$\varepsilon_i^{eq} = -(\kappa_{i1} B_{10}^1 + \kappa_{i2} B_{20}^1 + \kappa_{i3} B_{30}^1)\langle O_2^0 \rangle - (\kappa_{i1} B_{11}^1 + \kappa_{i2} B_{21}^1 + \kappa_{i3} B_{31}^1)\langle O_2^2 \rangle + (\kappa_{i1} I_1 \eta_1 \xi_1 + \kappa_{i2} I_2 \eta_2 \xi_2 + \kappa_{i3} I_3 \eta_3 \xi_3)\langle S_k \cdot S_l \rangle \tag{11}$$

and finally the equilibrium strain in (11) leads to the expression

$$\varepsilon_i^{eq} = \Pi_i^0 \langle O_2^0 \rangle + \Pi_i^2 \langle O_2^2 \rangle + \Gamma_i \langle S_k \cdot S_l \rangle \qquad i = 1, 2, 3 \tag{12}$$

where

$$\Pi_i^0 = -(\kappa_{i1} B_{10}^1 + \kappa_{i2} B_{20}^1 + \kappa_{i3} B_{30}^1) \tag{13a}$$

$$\Pi_i^2 = -(\kappa_{i1} B_{11}^1 + \kappa_{i2} B_{21}^1 + \kappa_{i3} B_{31}^1) \tag{13b}$$

$$\Gamma_i = \kappa_{i1} I_1 \eta_1 \xi_1 + \kappa_{i2} I_2 \eta_2 \xi_2 + \kappa_{i3} I_3 \eta_3 \xi_3. \tag{13c}$$

In (12), ε_1^{eq}, ε_2^{eq} and ε_3^{eq} correspond to the relative change in lattice parameters $\Delta c/c$, $\Delta a/a$ and $\Delta b/b$, respectively, for the orthorhombic symmetry, in the same way as that [12] defined previously. Therefore, the observed anisotropic thermal expansion below T_{tr} is determined in terms of the temperature behaviour of $\langle O_2^0 \rangle$, $\langle O_2^2 \rangle$ and $\langle S_k \cdot S_l \rangle$. The above expressions are similar to those [10, 12] obtained previously except the presence of the third term in (12).

4.3. Thermal expansion

From the present measurement of the lattice parameters for RZn_2 (R = Gd, Tb or Dy), the following features are obtained. (i) The anomalous thermal expansion is observed at the temperature which is associated with the appearance of magnetic orderings in all materials. (ii) $\Delta a/a$ for $GdZn_2$ is small and negative while those for $TbZn_2$ and $DyZn_2$ are both large and positive. (iii) $\Delta b/b$ for all RZn_2 is positive and it increases with varying R in the order R = Gd, Dy and Tb. (iv) $\Delta c/c$ for $GdZn_2$ is positive while those for $TbZn_2$ and $DyZn_2$ are small and large negative, respectively. (v) The absolute value of the change in c, $|\Delta c/c|$, below T_{tr} increases with the number of 4f electrons for $TbZn_2$ ($4f^8$ for Tb^{3+}) and $DyZn_2$ ($4f^9$ for Dy^{3+}). (vi) The magnitude of α_b above T_{tr} for RZn_2 decreases with varying R in the order R = Gd, Dy and Tb: $\alpha_b(GdZn_2) > \alpha_b(DyZn_2) > \alpha_b(TbZn_2)$. Here, T_{tr} represents collectively the magnetic transition temperature such as T_C or T_N. (vii) The value of α_c above T_{tr} is of nearly the same order of magnitude in all materials investigated. Since there are many unknown parameters in (13) which determines the coefficients Π_i^0, Π_i^2 and Γ_i, we will qualitatively discuss the features (i)–(vii) in terms of (12).

The magnetic structures for $TbZn_2$ and $DyZn_2$ have been proposed where the magnetic moments for Tb and Dy atoms are ferromagnetically aligned within the a–b plane while they are antiferromagnetically stacked along the c direction [3, 5]. This implies that in both cases of $TbZn_2$ and $DyZn_2$ the signs of ε_1^{eq}, ε_2^{eq} and ε_3^{eq} in the antiferromagnetic state are negative, positive and positive, respectively. This is consistent with the features (ii)–(iv) because in a band magnet the magnetic moments generally tend to become large when a cell volume expands. In comparison with the features (ii)–(iv) between ferromagnetic $GdZn_2$ and antiferromagnetic $TbZn_2$ and $DyZn_2$, the signs of ε_1^{eq} and ε_2^{eq} are opposite but that of ε_3^{eq} is the same. According to (12), the magnitude of ε_i^{eq} may be determined in terms of the relative magnitude of Π_i^0, Π_i^2 and Γ_i; if Π_i^0, Π_i^2 and Γ_i contribute positively, ε_i^{eq} may become large in comparison with that of the unstrained state and if they contribute negatively it may become small. In the case of $GdZn_2$, the anisotropic thermal expansion may be explained if the signs of coefficients in the third term of (12) are $\Gamma_1 > 0$, $\Gamma_2 < 0$ and

$\Gamma_3 > 0$. Here, the temperature dependence of $\langle S_k \cdot S_l \rangle$ is assumed to be a smooth function of T. Under this situation, it seems that the Gd moments in $GdZn_2$ are antiferromagnetically aligned along the a direction while they are ferromagnetically aligned along the b and c ones. Such an expected alignment of magnetic moments in $GdZn_2$ may be opposite to the one which has been proposed [3, 5] in $TbZn_2$ and $DyZn_2$. This means that the crystal field effect plays an important role in the stability of the antiferromagnetic alignments of magnetic moments for R atoms observed in the ground state for $TbZn_2$ and $DyZn_2$. From these situations for $TbZn_2$ and $DyZn_2$, it is considered that the magnitude of Π_i^0 and Π_2^2 ($i = 1, 2$) is significantly larger than that of the corresponding Γ_i. When we take into account the features (ii) and (iv), Π_1^0 and Π_1^2 may have opposite sign while Π_2^0 and Π_2^2 have the same one.

The $c(T)$ against T plots above T_{tr} for all materials investigated show a similar temperature dependence, as seen in figure 6. This suggests that the thermal expansion along the c direction in RZn_2 is due to a common origin. The meaning of the magnetoelastic coupling parameters B_{j0}^1 and B_{j1}^1 corresponds to the strain derivative of the second-order CF parameters, $B_{j0}^1 \sim \partial V_2^0/\partial \varepsilon_j$ and $B_{j1}^1 \sim \partial V_2^2/\partial \varepsilon_j$, respectively, which originate from two contributions, the ligands and the conduction electrons [24]. The former contribution is related to the electronic environment around the R^{3+} ion and the latter one the electronic states of the conduction band which are modified by the strain. The study [24] of the magnetoelasticity in cubic rare earth intermetallic compounds DyCu and DyZn has suggested that the main difference in the contribution of the conduction electrons to the magnetoelastic coefficients for these compounds is the hybridized mixing between the conduction band and d orbitals; the predominant type of d orbital for DyCu and DyZn is the t_{2g} and the e_g type, respectively. The latter d orbital points in the c direction when we take the quantization axis as the z one. From the structural feature in the $CeCu_2$-type structure, the shortest distance corresponds to one between R and Zn atoms along the c axis. Hence, it is considered that the magnetoelastic coefficient along the c axis in RZn_2 depends strongly on the modification of the conduction band through the e_g-type d orbital. Therefore, the opposite signs of Π_1^0 and Π_1^2 may be due to the modification of conduction band along the c axis. Under these situations, the feature (v) can be understood in terms of the change in the relative magnitude of Π_1^0 and Π_1^2 with the number of 4f electrons.

For supplementary information, the feature (i) means that the stability of the ferromagnetic state in $GdZn_2$ is mainly realized accompanying with small negative contraction along the a direction and large positive expansion along the b and c ones with decreasing T. The thermal expansion behaviour concerning $b(T)$ and $c(T)$ has been similarly reported in the antiferromagnet $GdCu_2$ [25]. However, in $GdCu_2$ $a(T < T_N)$ exhibits a large negative expansion as T decreases. This is remarkably different from the case of $GdZn_2$. In comparison with the θ_p–r plots for RZn_2 and RCu_2, the value of θ_p at r^b in $GdZn_2$ ($r^b = 3.96$ Å) may be small and negative while in $GdCu_2$ ($r^b = 3.79$ Å) it may be large and negative. This situation may be related to the small change in $a(T < T_C)$ of $GdZn_2$. In order to obtain further information on the crystal field and anisotropic thermal expansion, neutron diffraction studies of single-crystal RZn_2 are highly desired.

5. Conclusions

From the measurements of the powder x-ray diffraction patterns, the temperature dependence of the lattice parameters for RZn_2 (R = Gd, Tb and Dy) has shown the anisotropic thermal expansion behaviour along the a, b and c directions below T_{tr}. The positive expansion

of $b(T)$ below T_{tr} for all RZn_2 investigated is qualitatively explained in terms of the positive contribution to the thermal expansion which originates from the ferromagnetic exchange interaction between R atoms, together with the consideration of the θ_p–r plots. In comparison with the thermal expansion for RZn_2 (R = Gd, Tb and Dy), the present results indicate the necessity of taking into account the magnetic exchange contribution besides the crystal field one. From these situations, we proposed a phenomenological model in which the total free energy consists of the magnetoelastic, elastic and anisotropic Heisenberg-type exchange ones in order to explain the anisotropic thermal expansion in the magnetic states. On the basis of the present model, the present results concerning the different behaviour in $\Delta a/a$, $\Delta b/b$ and $\Delta c/c$ for RZn_2 could be explained in terms of the change in the signs of the phenomenological parameters Π_i^0, Π_i^2 and Γ_i.

Acknowledgment

A part of this work was carried out under the visiting researcher's program of the Institute for Materials Research, Tohoku University.

References

[1] Larson A C and Cromer D T 1961 *Acta Crystallogr.* **14** 73
[2] Debray D K, Wallace W E and Ryba E 1970 *J. Less-Common Met.* **22** 19
[3] Debray D, Sougi M and Meriel P 1972 *J. Chem. Phys.* **56** 4325
[4] Debray D, Wortmann B F and Methfessel S 1975 *Phys. Status Solidi* a **30** 713
[5] Ohashi M, Kitai T, Kaneko T, Yoshida H, Yamaguchi Y and Abe S 1990 *J. Magn. Magn. Mater.* **90 & 91** 585
[6] Abe S, Kaneko T, Ohashi M, Nakagawa Y and Kitai T 1992 *J. Magn. Magn. Mater.* **104–107** 1403
[7] Hashimoto Y, Fujii H, Fujiwara H and Okamoto T 1979 *J. Phys. Soc. Japan* **47** 67
[8] Hashimoto Y, Fujii H, Fujiwara H and Okamoto T 1979 *J. Phys. Soc. Japan* **47** 73
[9] Gratz E, Loewenhaupt M, Divis M, Steiner W, Bauer E, Pillmayr N, Müller M, Nowotny H and Frick B 1991 *J. Phys.: Condens. Matter* **3** 9297
[10] Gratz E, Rotter M, Lindbaum A, Müller H, Bauer E and Kirchmayr H 1993 *J. Phys.: Condens. Matter* **5** 567
[11] Gratz E, Pillmayr N, Bauer E, Müller H, Barbara B and Loewenhaupt M 1990 *J. Phys.: Condens. Matter* **2** 1485
[12] Diviš M, Lukáč P and Sovoboda P 1990 *J. Phys.: Condens. Matter* **2** 7569
[13] Šima V, Diviš M, Sovobada P, Smetana Z, Zajac S and Bischof J 1989 *J. Phys.: Condens. Matter* **1** 10153
[14] *Landolt–Börnstein New Series* 1989 Group III, vol 19, ed N S Madelung (Berlin: Springer) p 53
[15] Storm A R and Benson K E 1963 *Acta Crystallogr.* **16** 701
[16] Touloukian Y S, Kirby R K, Taylor R E and Desai P D 1977 *Thermophysical Properties of Matter* vol 12 (New York: Plenum) p 116
[17] Kitai T 1995 *J. Phys. Soc. Japan* to be submitted
[18] Hutchings M T 1964 *Solid State Physics* vol 16 (New York: Academic) p 227
[19] Zvezdin A K, Matveev V M, Muchin A A and Popov A I 1985 *Rare Earth Ions Magnetically Ordered Crystals* (Moscow: Nauka) p 98
[20] Nye J F 1957 *Physical Properties of Crystals* (Oxford: Clarendon) p 176
[21] Levy P M, Morin P and Schmitt D 1979 *Phys. Rev. Lett.* **42** 1417
[22] Lines M E and Jones E D 1965 *Phys. Rev.* **139** A1313
[23] Callen H B 1960 *Thermodynamics* (New York: Wiley) p 227
[24] Morin P and Schmitt D 1981 *Phys. Rev.* B **23** 2278
[25] Borombaev M K, Levitin R Z, Markosyan A S, Reimer V A, Sinitsyn E V and Smetana Z 1987 *Sov. Phys.–JETP* **66** 866